Carbohydrate Polymers 114 (2014) 269–278

Contents lists available at ScienceDirect

Carbohydrate Polymers

journal homepage: www.elsevier.com/locate/carbpol

Slow-released NPK fertilizer encapsulated by NaAlg-*g*-poly(AA-*co*-AAm)/MMT superabsorbent nanocomposite

Azam Rashidzadeh, Ali Olad*

Polymer Composite Research Laboratory, Department of Applied Chemistry, Faculty of Chemistry, University of Tabriz, 29 Bahman Street, Tabriz 5166616471, Iran

ARTICLE INFO

Article history:
Received 1 May 2014
Received in revised form 7 July 2014
Accepted 1 August 2014
Available online 17 August 2014

Keywords:
Superabsorbent
Nanocomposite
Montmorillonite
Water absorbency
Slow release

ABSTRACT

A novel slow released NPK fertilizer encapsulated by superabsorbent nanocomposite was prepared via in-situ free radical polymerization of sodium alginate, acrylic acid, acrylamide, and montmorillonite in the presence of fertilizer compounds. Evidence of grafting and component interactions, superabsorbent nanocomposite structure and morphology was obtained by a FT-IR, XRD and SEM techniques. The water absorbency behavior of superabsorbent nanocomposite was investigated. After those characterizations, the potential application was verified through the study of fertilizer release from prepared formulations. Results indicated that the presence of the montmorillonite caused the system to liberate the nutrient in a more controlled manner than that with the neat superabsorbent. The good slow release fertilizer property as well as good water retention capacity showed that this formulation is potentially viable for application in agriculture as a fertilizer carrier vehicle.

1. Introduction

Fertilizer is one of the vital input materials for the crop production. However, more than half of the applied amount of common fertilizers cannot reach the plant, but it is washed off by rain and irrigation water (Bajpai & Giri, 2002; Guo, Liu, Hu, Zhan, & Wu, 2005). This part of lost fertilizer not only causes large economic losses but also very serious environmental pollution. The overcoming of these shortcomings can be achieved with the use of slow release fertilizers (SRFs). SRFs are designed to gradually release fertilizers to plants at a rate to coincide with the nutrient requirement of a plant, while simultaneously reducing fertilizer loss (Liang & Liu, 2006; Teodorescu, Lungu, & Stanescu, 2009). At the same time, water is one of the main factors that limit the production of agriculture, so it is very important to use the water resource efficiently. Recently, investigation on the use of superabsorbent as water management materials for agricultural applications has attracted great attention. Superabsorbent polymers are cross linked hydrophilic polymers that can absorb water, saline solutions, or other liquids up to hundreds of times their own weight (Seetapan, Wongsawaeng, & Kiatkamjornwong, 2011). In agricultural uses, especially in arid areas, the use of superabsorbents causes to increase the water-holding capacity and therefore the fertility of the soil (Zohuriaan-Mehr, Omidian, Doroudiani, & Kabiri, 2010). From the application point of view, the combination of superabsorbents and SRFs may improve the water-holding capacity and nutrient retention of sandy soils and also increase the soil's aeration and microbial activity, and mitigate at the same time the environmental impact from water-soluble fertilizers, lower frequency of irrigation (El-Rehim, Hegazy, & El-Mohdy, 2004). The majority of superabsorbents are made from synthetic hydrophilic polymers such as poly (acrylic acid) or its copolymer with poly (acrylamide) (Ni, Liu, Lü, Xie, & Wang, 2010). However, because of poor degradability in soil and their accumulation over time, the demand for using environmentally safe, degradable superabsorbent is continuously increasing. Alginate, a polysaccharide obtained from brown algae, due to its biodegradability and low cost has recently gained great attention in controlled release of drugs (Wang, Hu, Du, & Kennedy, 2010; Wang, Zhang, Hu, Yang, & Du, 2007) and agrochemicals (Liu, Wu, & Chang, 2008). Alginate-based superabsorbents prepared by graft polymerization with acrylic acid and acryl amide monomers onto a chain of alginate has been widely used in agriculture (El-Rehim & Hassan, 2006). Nevertheless, in spite of the advantages of superabsorbent application as fertilizer carriers, the high price of the product in the market makes its application unfeasible. To solve the high cost problem, one of the alternatives is to form a nanocomposite with clay minerals such as montmorillonite (Wu, Wei, Lin, & Lin, 2003), attapulgite (Liang & Liu, 2006), and kaolin (Hussien et al., 2012) in high proportions. This introduction not only reduces the final cost of the product

* Corresponding author. Tel.: +98 411 3393164; fax: +98 411 3340191.
E-mail address: a.olad@yahoo.com (A. Olad).

http://dx.doi.org/10.1016/j.carbpol.2014.08.010
0144-8617/

Table 1
Concentration of MBA, APS and MMT in superabsorbent samples.

Sample	MBA (wt%)	APS (wt%)	MMT (wt%)
Superabsorbent samples	0.127	1.2	0
	0.375	1.2	0
	0.75	1.2	0
	1.25	1.2	0
Superabsorbent nanocomposite samples	0.75	1.2	5
	0.75	1.2	10
	0.75	1.2	15
	0.75	1.2	20

drastically but also improves swelling property, gel strengths and mechanical and thermal stability (Schexnailder & Schmidt, 2009). Moreover, it has been proved that the inclusion of inorganic clays into hydrogels decreases the release rate of fertilizer from slow-release formulation (Liang & Liu, 2006). Poly acrylamide/methyl cellulose/montmorillonite nanocomposite hydrogel has been used for slow release of urea fertilizer (Bortolin, Aouada, Mattoso, & Ribeiro, 2013). To the best of our knowledge, SRF formulation has not been prepared by in-situ polymerization of monomers in the presence of fertilizer solution. Also the fertilizer slow release property of prepared formulation based on both montmorillonite and alginate-*g*-poly(acrylic acid-*co*-acrylamide) (Hyd) superabsorbent has not been investigated so far. Therefore, in the present work we attempted to synthesis a novel SRF superabsorbent nanocomposite and investigate its water absorbency and fertilizer slow release properties.

2. Experimental

2.1. Materials

Acrylic acid (AA), acrylamide (AAm), *N*,*N*′-methylene bisacrylamide (MBA), ammonium persulfate (APS), urea, potassium dihydrogen phosphate and ammonium dihydrogen phosphate were purchased from Merck. Sodium alginate (NaAlg), (viscosity of 5.0–40.0 cps for a 1% solution at 25 °C), was purchased from Sigma-Aldrich and was used without further purification. Sodium montmorillonite (MMT), (specific surface area = 20–40 m^2/g, cation exchange capacity = 30 meq/100 g), was obtained from Sigma-Aldrich. Other agents were all analytical grade and all solutions were prepared with distilled water.

2.2. Preparation of slow released NPK fertilizer formulation

2.2.1. Preparation of Hyd/MMT superabsorbent nanocomposite

NaAlg solution (3%, w/v) in distilled water was prepared under constant stirring. Then the MMT suspension (5–20 wt%, with respect to NaAlg) was added into NaAlg solution while agitation for 6 h. Thereafter, the solution was charged in a four necked flask equipped with a mechanical stirrer, reflux condenser, a thermometer, and a nitrogen line. After being purged with nitrogen gas for 30 min to get rid of dissolved oxygen in the solution, and heating to 60 °C in a water bath, the APS solution (1.2 wt%) as initiator and 6 g of AAm were added. Afterwards mixture solution of AA (7 ml) and MBA (0.1–1.25% wt%, with respect to monomers) was charged into the flask dropwise. The water bath was heated slowly to 70 °C and kept for 4 h to complete polymerization. The resulting gel product was dried in a vacuum oven at 70 °C and then was grounded and passed through 40–80 mesh sieves. The preparation procedure of Hyd superabsorbent is similar to that of the Hyd/MMT superabsorbent nanocomposite except without the addition of MMT. Table 1 shows the concentration of the materials used in preparation of superabsorbent samples.

2.2.2. Preparation of Hyd/MMT/NPK formulation

In-situ polymerization method was used to encapsulate NPK fertilizer into the superabsorbent nanocomposite. NPK fertilizer composed of urea (10 g), ammonium dihydrogen phosphate (5 g) and potassium dihydrogen phosphate (5 g) was dissolved in distilled water and then was mixed with NaAlg solution under constant stirring. In continue a similar procedure was adopted to synthesize the Hyd/MMT/NPK formulation.

2.3. Water absorbency measurements

To obtain cylindrical shapes samples for water absorbency measurements, superabsorbent samples were synthesized in plastic tubes of 5 mm internal diameters and about 200 mm long and dried at 70 °C for 4 h in an oven. To investigate water absorbency, about 0.1 g of the samples was immersed in the distilled water at room temperature. Then at regular time intervals the weight of the swollen samples was determined. Each experiment was performed twice. The equilibrium water absorbency Q_{eq} (g/g) was calculated by using the following equation:

$$Q_{eq}(g/g) = \frac{W_s - W_d}{W_d} \quad (1)$$

where W_s (g) is the weight of the swollen sample, and W_d (g) is the initial weight of the dry sample.

2.4. Slow release behavior of Hyd/MMT/NPK superabsorbent nanocomposite

2.4.1. Slow release behavior in water

For release experiments of NPK Fertilizer encapsulated by superabsorbent nanocomposite, 1 g of Hyd/MMT/NPK sample was immersed into 100 ml of distilled water. At certain time intervals, 10 ml solution was sampled for fertilizer determination, and an additional 10 ml of distilled water was added into the beaker to maintain a constant amount of solvent. All the release experiments were carried out twice and the mean value was used for plotting. The fertilizer concentration was determined using digital conductivity meter, and cumulative release was obtained by the following formula:

$$E = \frac{V_E \sum_1^{n-1} C_i + V_0 C_n}{m_0} \times 100 \quad (2)$$

where E is the accumulative release (%) of fertilizer, V_E is the sampling volume, V_0 is the initial volume of release media, C_i and C_n are the fertilizer concentrations (mg/ml), i and n are the sampling times, and m_0 is the mass of fertilizer in the formulation samples (mg).

2.4.2. Slow release behavior in soil

To study release of NPK Fertilizer in soil, 1 g of dry sample of Hyd/MMT/NPK was well-mixed with 100 g of dry sandy soil (below 25 mesh). Then the mixture was filled into homemade glass column equipped with ceramic membrane and valve. Next, 45 ml water was added to soil column until it reached the soil–water saturation point. The moisture content in the column was maintained approximately constant throughout the period of study by adding water (25 ml). At certain time intervals, 10 ml of the water of the soil was collected and the fertilizer content in the solutions was tested.

2.5. Water retention behavior of the soil

1 g of Hyd/MMT/NPK was well mixed with 100 g of dry soil (below 25 mesh) and placed in a plastic beaker, and then 50 ml of distilled water was slowly added into the beaker and weighed (W_o). A control experiment without Hyd/MMT/NPK was also carried out

(W). The beaker was maintained at room temperature and weighed every day (W_t) over a period of 30 days. The water retention (%WR) of soil was calculated from the following equation:

$$WR\% = \frac{W_t - W}{W_o - W} \times 100 \quad (3)$$

3. Results and discussion

3.1. Superabsorbent preparation mechanism

Hyd/MMT superabsorbent nanocomposite was prepared through graft copolymerization of acrylic acid and acrylamide onto sodium alginate in the presence of MBA as crosslinking agent and montmorillonite clay. The proposed mechanism for preparation of superabsorbent nanocomposite is outlined in Fig. 1. The mechanism of superabsorbent nanocomposite preparation has been discussed in detail in our previous work (Rashidzadeh, Olad, Salari, & Reyhanitabar, 2014). As it is clear, the MMT clay may act as a crosslinking agent to form superabsorbent network.

3.2. Characterization

3.2.1. FT-IR spectra

The FT-IR spectra of the MMT, NaAlg, Hyd, Hyd/MMT, Hyd/MMT/NPK and pure NPK fertilizer are shown in Fig. 2a. In FT-IR spectra of MMT, the strong absorption peaks at 1029 cm^{-1} (Si—O bond stretching), 522 cm^{-1} (Al—O bond stretching) and 462 cm^{-1} (Mg—O bond stretching) are characteristic peaks of MMT. The absorption peak at 1633 cm^{-1} was assigned to H—O—H deformation and the bands at 3421 and 3622 cm^{-1} are related to stretching vibration of structural O—H and N—H groups of MMT, respectively (Olad & Rashidzadeh, 2012). In FT-IR spectra of NaAlg the characteristic peaks of NaAlg can be seen at around 1640 cm^{-1} and 1419 cm^{-1} wave numbers (carboxylate stretching vibrations), a broad band at 3418 cm^{-1} (hydroxyl groups stretching absorption), and the bands between 900 and 1200 cm^{-1} (O—C—O stretching of

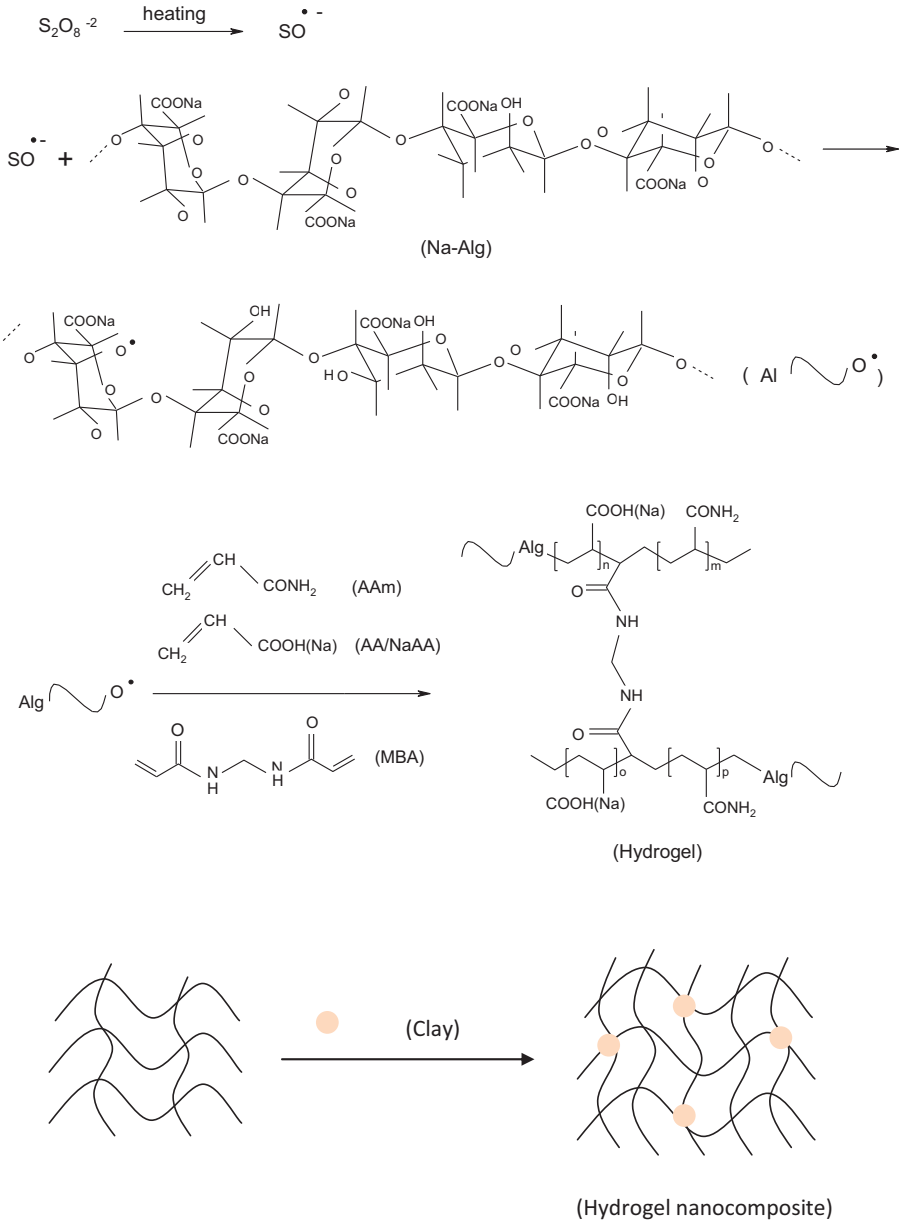

Fig. 1. Proposed reaction mechanism for synthesis of superabsorbent nanocomposite

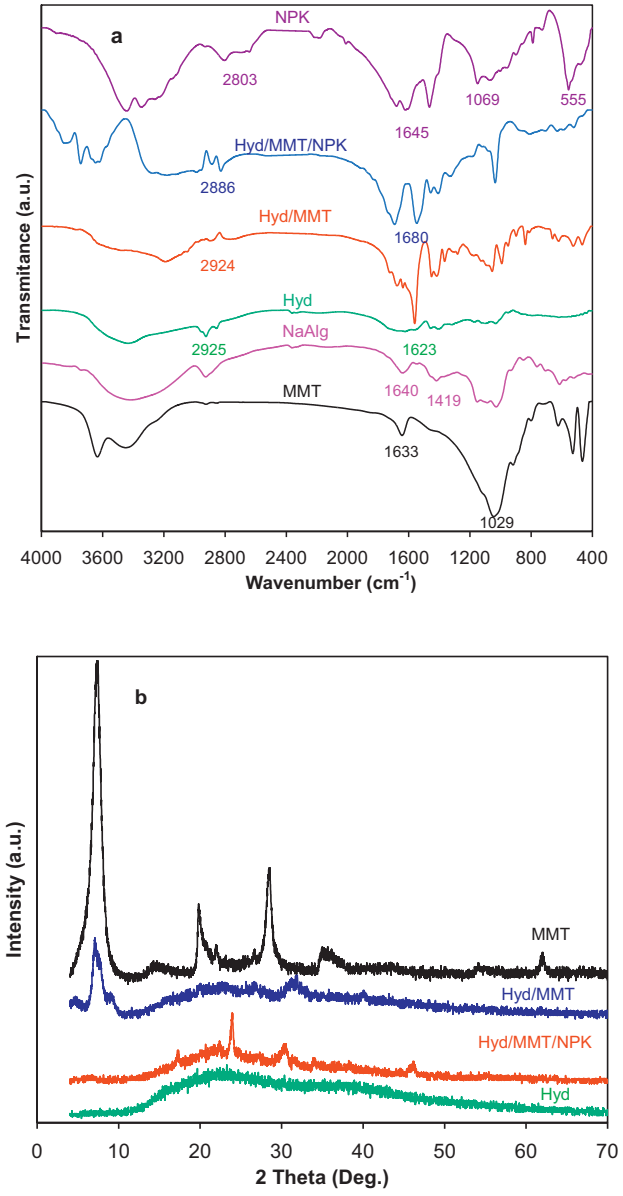

Fig. 2. The FT-IR spectra of MMT, NaAlg, Hyd, Hyd/MMT, Hyd/MMT/NPK, pure NPK fertilizer (a) and XRD patterns of MMT, Hyd, Hyd/MMT, Hyd/MMT/NPK (b) (AAm, 6 g; AA, 7 ml; neutralization degree, 70%; APS, 1.2 wt%; MBA, 0.75 wt%; MMT, 15 wt%; NPK fertilizer, 20 g; reaction temperature, 70 °C).

ether groups and —C—O stretching of alcoholic groups) (Pourjavadi, Ghasemzadeh, & Soleyman, 2007). In FT-IR spectra of Hyd, Hyd/MMT, Hyd/MMT/NPK, the bands at 1623 cm^{-1}, 1676 cm^{-1} and 1680 cm^{-1} are related to the overlapped stretching vibration of the carbonyl groups of AA and AAm as well as the N—H bending (Owens et al., 2007). Also, the intense and sharp bands between 3300 cm^{-1} and 3500 cm^{-1} are due to the overlapping the absorption bands of O—H and stretching vibrations of N—H groups. The bands appeared at 2886 cm^{-1} to 2925 cm^{-1} are due to the combined stretching of CH_2 groups in both AA and AAm in superabsorbent structure. The peak of MMT at 1029 cm^{-1}, due to Si—O group, is also observed with slight shift in Hyd/MMT and Hyd/MMT/NPK which indicates the incorporation of the MMT into the superabsorbent. It is worth to mention that the shift of absorbtion bands of carbonyl from 1632 cm^{-1} (in Hyd) to around 1676 cm^{-1} (in Hyd/MMT) and 1692 cm^{-1} (in Hyd/MMT/NPK) might be due to the formation of hydrogen bonding between the carboxyl and carbonyl groups of the hydrogel materials and the hydroxyl groups of Al—OH and Si—OH in MMT. Furthermore, the absorption bands of O—C—O stretching of the ether groups and the —C—O stretching of alcoholic groups of NaAlg disappeared in the FT-IR spectrum of superabsorbent samples suggesting the grafting reaction of AA and AAm on NaAlg (Hua & Wang, 2009). In the FT-IR spectrum of pure NPK fertilizer the peaks between 3300 and 3500 cm^{-1} are due to stretching modes of O—H and N—H in NPK fertilizer consisting of urea, potassium dihydrogen phosphate and ammonium dihydrogen phosphate. The peaks at about 2803 cm^{-1} is corresponded to the O—H stretching, 1465 cm^{-1} is due to P=O stretching, 1150 cm^{-1} is related to P—OH stretching, 1069 cm^{-1} is attributed to the HO—P—OH bending (Chaki, Deshpande, Tailor, Chaudhary, & Mahato, 2012; Muley, 2012). Also, the band of PO_4 vibration is appeared at 555 cm^{-1}. The peaks between 700 cm^{-1} to 900 cm^{-1} are due to the O—N=P and $—ONO_2$ bond vibration in ammonium dihydrogen phosphate. Also a sharp peak at 1600 to 1700 cm^{-1} is assigned to the C=O stretching mode related to urea (Emrani, Davoodnia, & Tavakoli-Hoseini, 2011; Jung, Czarnik-Matusewicz, & Kim, 2004; Rahman, Das, Miah, & Ahmad, 2008). The FT-IR spectrum of the Hyd/MMT/NPK in comparison to Hyd/MMT shows the corresponding peaks of NPK fertilizer with slight shift in place. Therefore it can be concluded that NPK fertilizer is successfully encapsulated in Hyd/MMT/NPK superabsorbent nanocomposite.

3.2.2. XRD patterns

Fig. 2b shows the XRD patterns of pristine MMT, Hyd, Hyd/MMT, and Hyd/MMT/NPK. The crystalline peak of MMT is observed at about 7.33° corresponds to the periodicity in the direction of (0 0 1) of the MMT (Wang, Nakajima, Manias, & Chung, 2003). In the case of Hyd/MMT, the (0 0 1) peak is shifted toward a lower angle (7.15°). This results from intercalation of hydrogel between the clay layers which lead to increase the *d*-spacing in the direction of (0 0 1) for MMT from 12.019 Å to 12.351 Å. The slight shift in place of peaks indicated the intercalated structure of Hyd/MMT formulation. The XRD patterns of Hyd show weak broad peaks at $2\theta = 22°$ and $2\theta = 38°$ because of its amorphous structure of hydrogel with low crystallinity. In contrast Hyd/MMT had the typical crystallite reflections associated with the montmorillonite component. Presence of the peaks related to the MMT in the XRD pattern recorded for hydrogel nanocomposite, confirms the presence of MMT in the nanocomposite composition. In the case of Hyd/MMT/NPK, the diffraction peak related to montmorillonite is disappeared which is an indicative of exfoliated structure. In exfoliated structures no more diffraction peaks are visible in the XRD diffractograms either because of a too large spacing between the layers or because the nanocomposite does not present ordering. The extensive layer separation associated with exfoliated structures disrupts the coherent layer stacking and results in a featureless diffraction pattern (Pavlidou & Papaspyrides, 2008).

3.2.3. Investigation of surface morphology

The surface morphologies of Hyd (a), Hyd/MMT (b) and Hyd/MMT/NPK (c–e) were investigated using scanning electron microscopy (SEM). Fig. 3a shows the SEM image of freeze-dried Hyd superabsorbent sample with 0.75 wt% MBA. A homogeneous, high porous with honeycomb-like structure with pore sizes in the range of several tens of microns was clearly shown for Hyd sample, which seemed to indicate a higher absorbtion of water to the superabsorbent. In comparison the SEM micrograph of freeze-dried Hyd/MMT in Fig. 3b is composed of more pores with open channels. By addition of MMT, due to the montmorillonite role as the physical crosslinking agent, the homogeneity as well as the pore size structure of the copolymer decreases, but the number of pores and channels increases and, consequently, the Hyd/MMT superabsorbent nanocomposite swelling was expected to increase. SEM micrograph of freeze-dried Hyd/MMT/NPK can be seen in Fig. 3c.

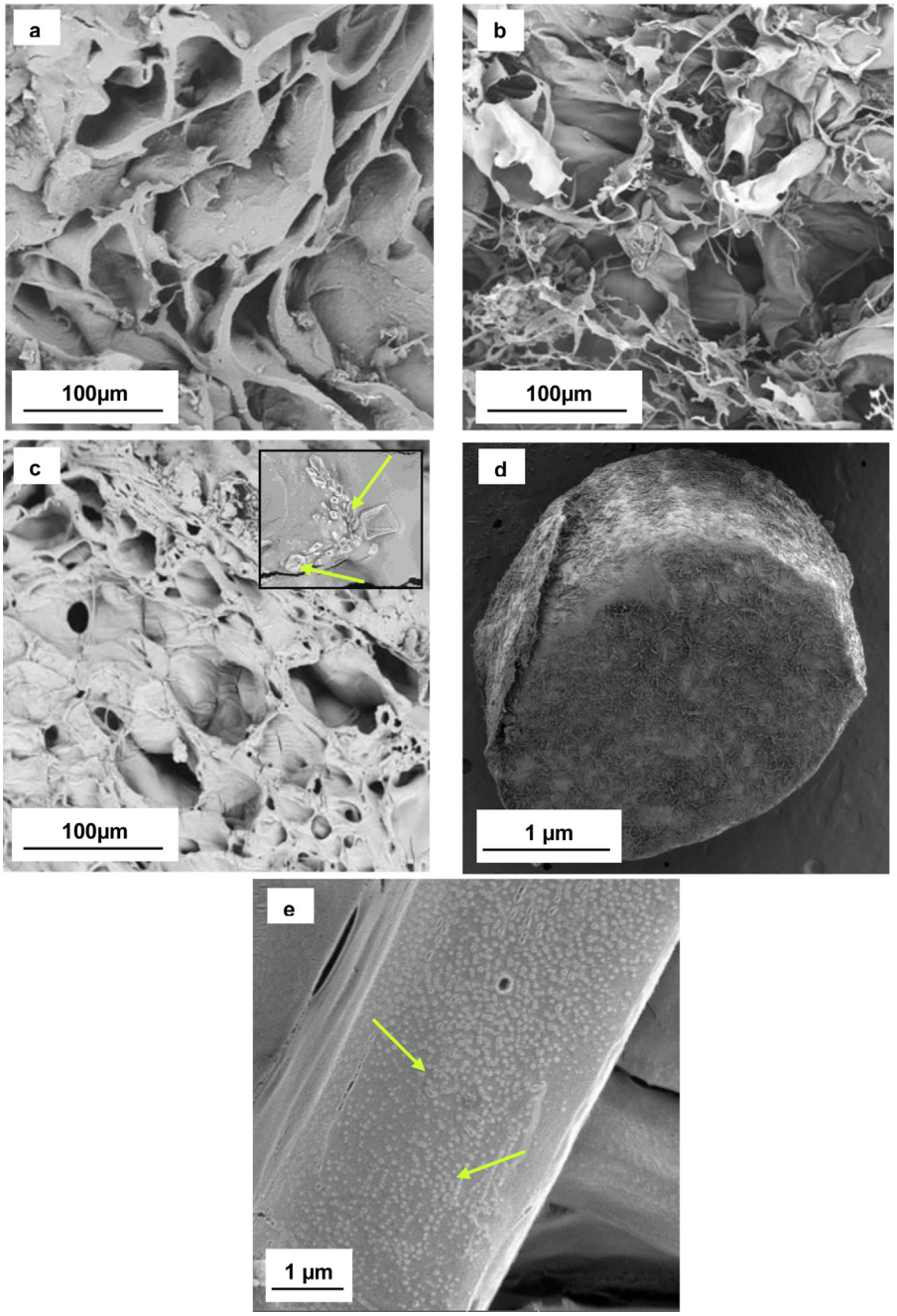

Fig. 3. SEM micrographs of (a) Hyd, (b) Hyd/MMT, (c) freeze-dried Hyd/MMT/NPK, and ((d)–(e)) oven dried cylindered Hyd/MMT/NPK (reaction conditions same as in Fig. 2)

As it is evident, NPK fertilizer is homogeneously deposited on to the walls of the pores of Hyd/MMT. In the higher magnification the tetrahedral urea crystals as well as potassium dihydrogen phosphate and ammonium dihydrogen phosphate crystals can be seen on the surface of Hyd/MMT. As it is evident, highly porous structure of Hyd/MMT/NPK formed by addition of montmorillonite to the pure superabsorbent can absorb large amount of water and can meanwhile control the release of fertilizer from it. The SEM images of oven dried cylindered Hyd/MMT/NPK sample were shown in Fig. 3d–e. The fertilizer crystals made up of a mixture of urea, ammonium dihydrogen phosphate and potassium dihydrogen phosphate are homogenously dispersed on the Hyd/MMT Hyd/MMT/NPK sample surface (Fig. 3d). Furthermore, as was shown in higher magnification image (Fig. 3e), the surface of the Hyd/MMT/NPK was covered by small urea crystals around 50 nm in size. The characteristics of surface morphology are very significant for water absorbency of superabsorbent nanocomposite. Therefore, when Hyd/MMT/NPK sample is dipped in water, it can absorb water quickly to form a swollen hydrogel, which is responsible for the water retention property of Hyd/MMT/NPK sample.

3.3. Water absorbency studies

Examination of water absorbency behavior of superabsorbents is essential for many applications like agriculture.

3.3.1. Effect of crosslinker content on the water absorbency behavior

The crosslinking agent plays an important role in the formation of three-dimensional network structures of superabsorbents in the polymerization process. Superabsorbents with different MBA contents, according to Table 1, were prepared. Then the effect of

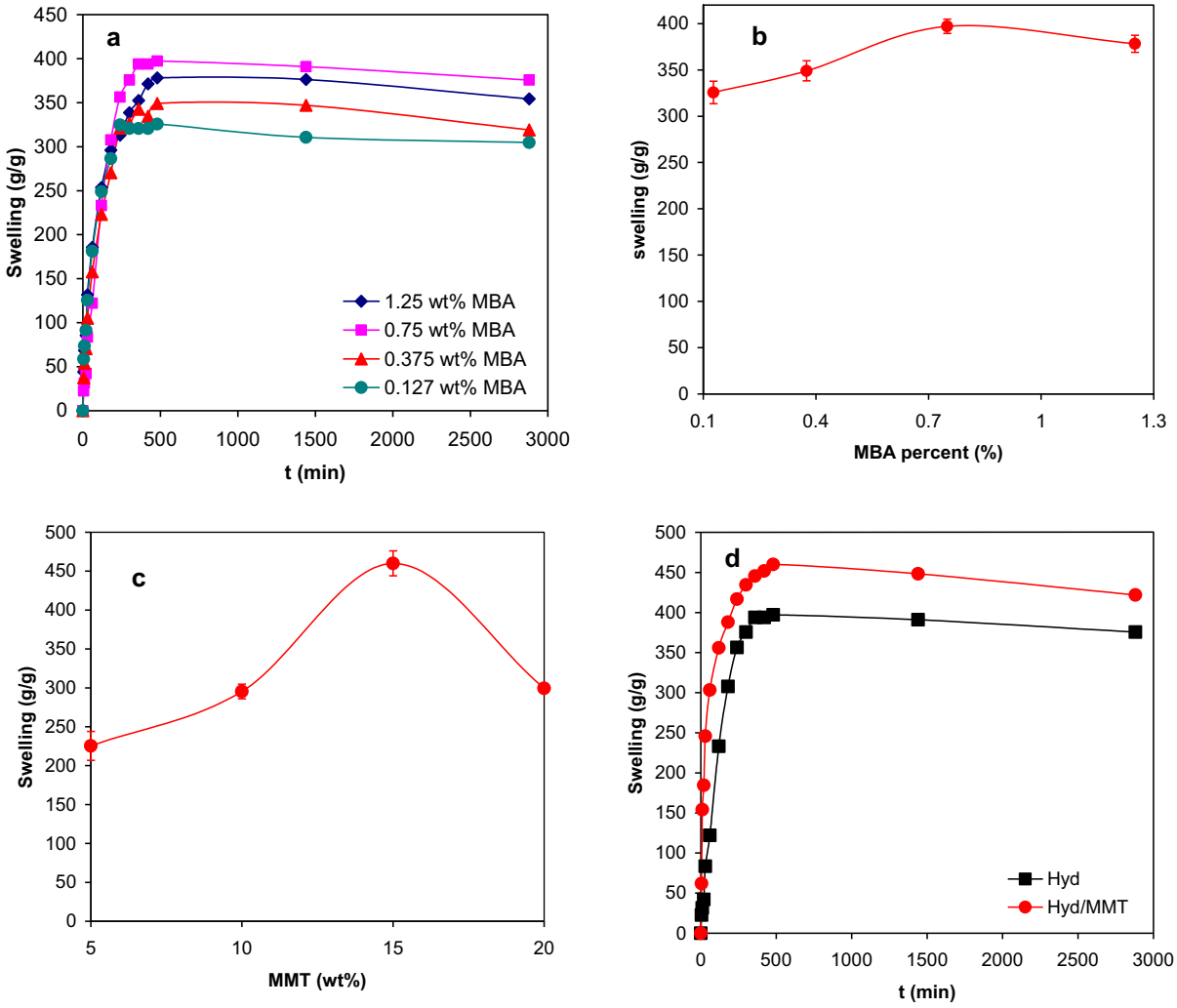

Fig. 4. The effect of MBA content on the water absorbency ((a) and (b)) and the effect of MMT content on the water absorbency ((c) and (d))

MBA content as crosslinking agent on the water absorbency of superabsorbents was investigated. Fig. 4a and b shows the effect of MBA content on the water absorbency of prepared superabsorbents with different MBA content. As one can easily see from Fig. 4a, the observed trends in the water absorbency kinetics for all samples with different MBA content are very similar. Initially, the rate of water uptake sharply increases, and then followed by a slower rate until the equilibrium water absorbency is reached at 480 min. In Fig. 4b, the equilibrium water absorbency values versus wt% MBA was plotted. As it was clear from Fig. 4b, the highest water absorbency of 397.2 (g/g) for the superabsorbent samples occurs at 0.75 wt% MBA content. When the MBA is lower than 0.75 wt%, water absorbency decreases because of increasing the soluble materials of superabsorbent. A further increase in the MBA content results in increase the crosslinking density of the superabsorbent network which in turn decrease the space among the grids of the superabsorbent network for holding of water. This would make it more difficult for the network to be swollen by water, which was responsible for the decrease in water absorbency. Therefore the optimum amount of MBA is 0.75 wt% which gives higher water absorbency to superabsorbent.

3.3.2. *Effect of MMT content on the water absorbency behavior*

The effect of MMT content on the water absorbency of superabsorbent nanocomposite was investigated using superabsorbent nanocomposite samples with different MMT contents, according to Table 1, and the results was presented in Fig. 4c and d. As can be seen from Fig. 4c, upon introducing MMT from 5 wt% to 15 wt%, the superabsorbent exhibited an increase in the water absorbency from 225.3 (g/g) to 460.016 (g/g). This phenomenon could be attributed to reaction between MMT and superabsorbent. In other word, because of special crystalline structure of MMT with negative surface charge, high repulsive forces between COO^- groups of superabsorbent and negative surface charge of MMT resulted in increased expansion of the superabsorbent network and higher water absorbency. On the other hand, the swelling of superabsorbent nanocomposite decreased to 299.4 (g/g) for higher MMT loading from 15 to 20 wt%. The reduction of water absorbency in the presence of more MMT was due to role of MMT as the physical crosslinking agent. When the amount of MMT is low, lower crosslinking density with smaller MMT content is created. However, when MMT content was higher than 15%, the generation of more crosslinking points restricts the movement of polymer chains (Wu & Liu, 2007). Besides that, NaAlg-*g*-Poly(AA-*co*-AAm) superabsorbent is liable for the water absorbency of nanocomposite. The higher the MMT content, the lower the superabsorbent in the nanocomposite and consequently the water absorbency of the superabsorbent nanocomposite is lower. Fig. 4d shows that the water absorbency of Hyd/MMT is significantly higher than that of the superabsorbent without MMT. According to the SEM analysis, the introduced MMT generated a loose and more porous material in comparison with pure superabsorbent. This structure of material

is convenient for the penetration of water molecules into the polymeric network, and then may be of benefit to water absorbency of the superabsorbent nanocomposites.

3.3.3. Effect of pH on the swelling

The swelling behavior of the superabsorbent samples at various pH values between 2.0 and 12.0 was shown in Fig. 5. As shown in Fig. 5a, the swelling of the superabsorbents was increased with increasing pH from 2 to 5, then it become stable in the pH region of 5 to 9, but it was decreased in the higher pH values from 9 to 12. The behavior of Hyd/MMT in various pH values was schematically shown in Fig. 5b. The maximum water absorbency of the Hyd/MMT was achieved at pH 5. In an acidic solution, because of the presence of high concentration of H^+, most of the carboxylate anions are protonated, so efficient anion–anion electrostatic repulsion was prevented. At pH values from 5 to 9, all the —COOH groups were converted to $—COO^-$, and this resulted in high anion–anion repulsion and high swelling capacity. At pH values higher than 9 the swelling of Hyd/MMT decreased. This is due to the presence of Na^+ cations from NaOH in the solution, which shields the

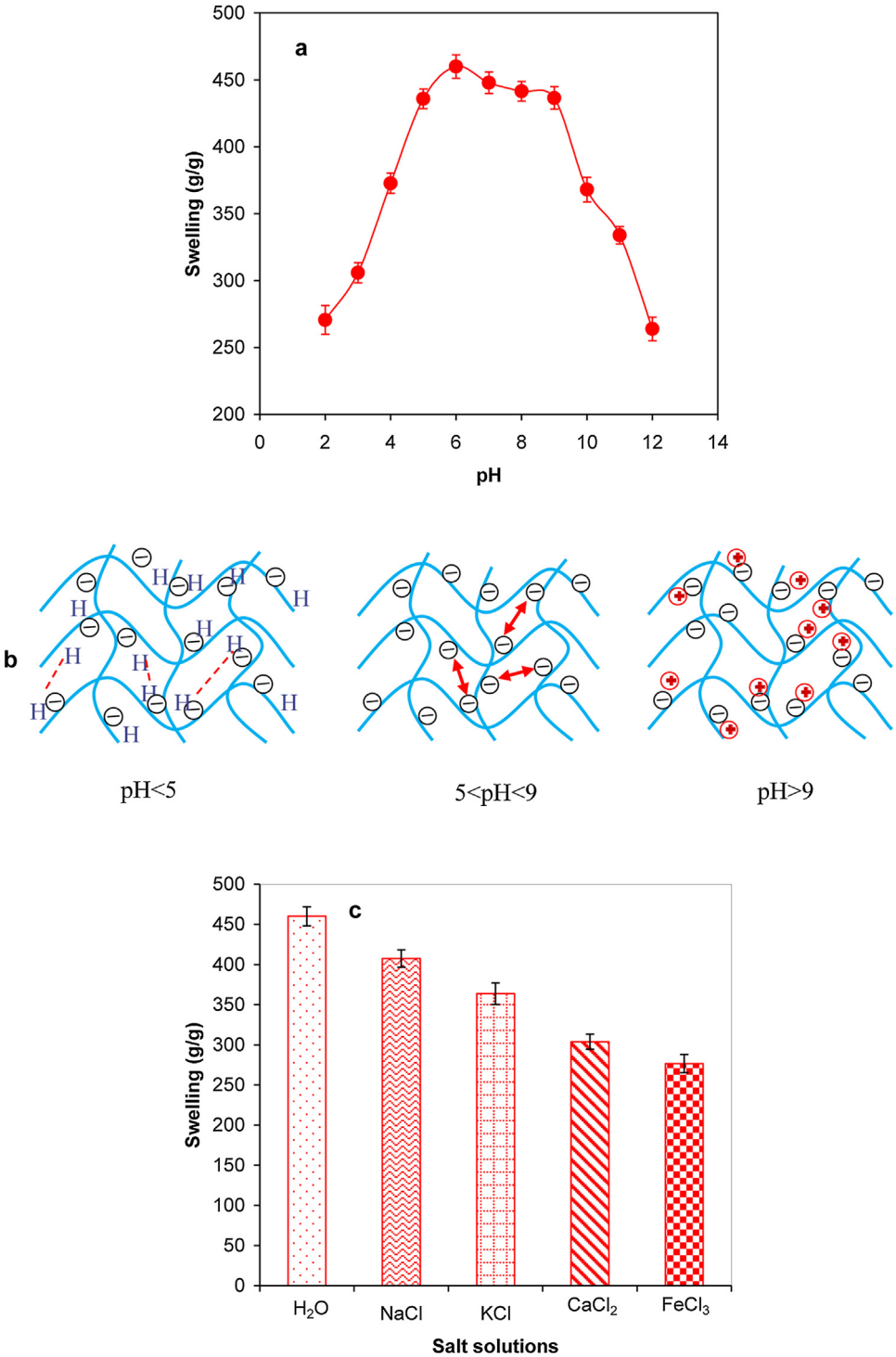

Fig. 5. The effect of solution pH on the water absorbency (a), the schematic behavior of superabsorbent nanocomposite in various pH values (b), and the effect of various salt solutions on the water absorbency (c)

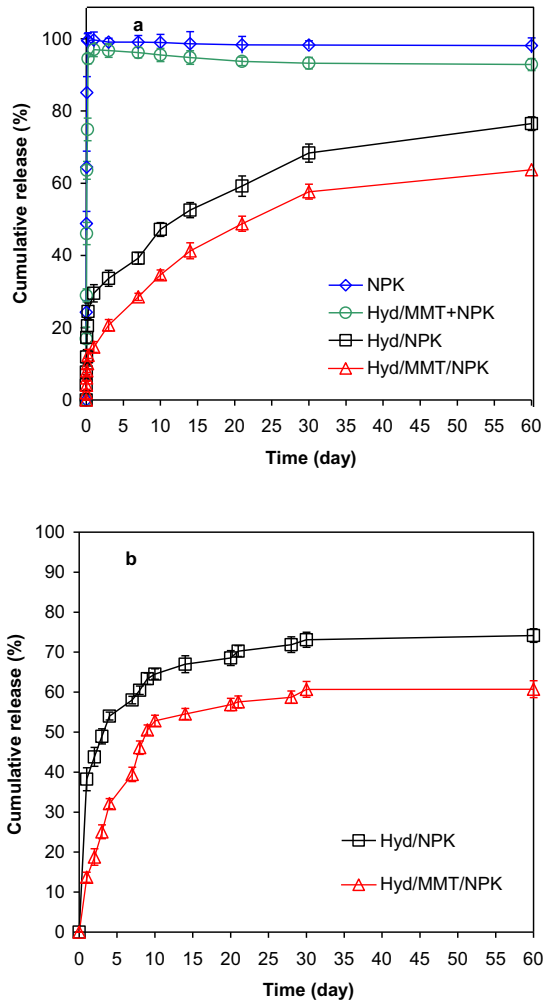

Fig. 6. Fertilizer release behaviors of NPK fertilizer, Hyd/NPK, Hyd/MMT + NPK, and Hyd/MMT/NPK in water (a), fertilizer release behaviors of Hyd/NPK and Hyd/MMT/NPK in soil (b)

—COO^- groups and prevented perfect anion–anion repulsion. With environment pH enhancement, accumulation of carboxylic ions inside the Hyd/MMT network increases the water discharge from it (due to weakening hydrogen bonds between water molecules and carboxylic groups) and the Hyd/MMT shrinks.

3.3.4. Effect of salt solutions on the swelling property

Examination of swelling behavior of Hyd/MMT superabsorbents in NaCl, KCl, $CaCl_2$ and $FeCl_3$ saline solutions is shown in Fig. 6c. According to Fig. 5c, the swelling of Hyd/MMT in all salt solutions is significantly lower than that of the values in distilled water. This phenomenon is related to osmotic pressure and elasticity of the superabsorbent network. Also, because of charge screening effect or shielding of carboxylate anions with monovalent cations, expansion of the superabsorbent network due to low repulsive forces in superabsorbent and decreased osmotic pressure decreases (Pourjavadi et al., 2007). As can be seen from Fig. 5c, the swelling of Hyd/MMT in salt solutions is in the order of $Na^+ > K^+ > Ca^{2+} > Fe^{3+}$, respectively. In the case of multivalent cations like Ca^{2+} and Fe^{3+}, formation of complexes with carboxylate groups of superabsorbent resulted in creation of crosslinking points which avoided the expansion of superabsorbent and decrease the swelling of the superabsorbent. Moreover, by increasing the charge of cation from divalent (Ca^{2+}) to trivalent cations (Fe^{3+}), degree of crosslinking due to the increasing electrostatic attraction between anionic sites of superabsorbents and Fe^{3+} cations increased and swelling is consequently decreased (Bao, Ma, & Li, 2011; Marandi, Mahdavinia, & Ghafary, 2011).

3.4. Fertilizer release

In order to investigate the release of fertilizer, conductivity measurements, reflecting the total concentration of fertilizers, were performed as a function of time. Fig. 6a represents the fertilizer release behaviors of untreated fertilizer (NPK), superabsorbent encapsulated fertilizer (Hyd/NPK), untreated fertilizer and superabsorbent nanocomposite mixture (Hyd/MMT + NPK), and SRF superabsorbent nanocomposite (Hyd/MMT/NPK) in water. Complete release of fertilizers in NPK fertilizer was released within 4 h as shown in Fig. 6a. The fertilizer release rate from NPK fertilizer mixed with superabsorbent nanocomposite decreased compared with that of NPK fertilizer, in agreement with the results of other works (Wu & Liu, 2008) but it was still obviously higher than that of Hyd/MMT/NPK. A low concentration of fertilizer was slowly released to the release medium from Hyd/NPK and Hyd/MMT/NPK samples. It could be seen from Fig. 6a that the release of fertilizer from Hyd/NPK is 29.53%, 39.23% and 68.34% in the first day, one week and one month, respectively. In contrast, in the case of Hyd/MMT/NPK release of fertilizer is 14.66% on the first day, 28.54% on one week, and 57.66% on one month. As shown in Fig. 6a, the fertilizer in Hyd/MMT/NPK possessed excellent slow-release property. Fig. 6b shows the fertilizer release behaviors of Hyd/NPK and Hyd/MMT/NPK in soil. As shown in Fig. 6b, the fertilizers in Hyd/NPK and Hyd/MMT/NPK released 38.23%, 58.01%, 73.1% and 13.7%, 39.42%, 60.69% within 1, 7, and 30 days, respectively. Slower release of fertilizer from Hyd/MMT/NPK than Hyd/NPK can be related to highly porous structure of Hyd/MMT/NPK formulation. NPK fertilizer encapsulated in Hyd/MMT/NPK formulation can be released out of formulation slowly, due to the maze or tortuous path created by montmorillonite layers which retards the diffusion of fertilizer through the Hyd/MMT superabsorbent to the medium. The addition of montmorillonite to the pure superabsorbent not only causes porous structure in superabsorbent nanocomposite but also controls the release of fertilizer from it. With the sum of fertilizer release lower than 15% on the first day and not above 75% on the thirtieth day, this indicated that the slow release character of the Hyd/MMT/NPK prepared in this work agreed with the standard of slow release fertilizers of the Committee of European Normalization (CEN) (Trenkel & Association, 1997).

The fertilizer release mechanism of Hyd/MMT/NPK superabsorbent nanocomposite in soil could be illustrated as followings: The fertilizer encapsulated in Hyd/MMT/NPK formulation is composed of urea, potassium dihydrogen phosphate and ammonium dihydrogen phosphate which can easily dissolve in water, and therefore the fertilizer is released out to the medium. At first, after being added into soil, Hyd/MMT/NPK would be slowly swollen by the water in soil and transformed to hydrogel. Then the fertilizer encapsulated into Hyd/MMT/NPK formulation or on its surface could be slowly dissolved. In the next stage, the fertilizer would slowly be released into the soil through the superabsorbent nanocomposite with the dynamic exchange of the water in the hydrogel and the water in the soil. In this stage, diffusion would be the release rate-limiting step. With the increase of swelling ratio of superabsorbent nanocomposite, the aperture size of the three-dimensional network of Hyd/MMT/NPK increases which benefits the diffusion of the fertilizer into the soil. This phenomenon continues until the equilibrium swelling ratio of superabsorbent nanocomposite. After that the fertilizer release into the soil decreases and becomes constant. The formulations developed within this work display several advantages over the SRFs

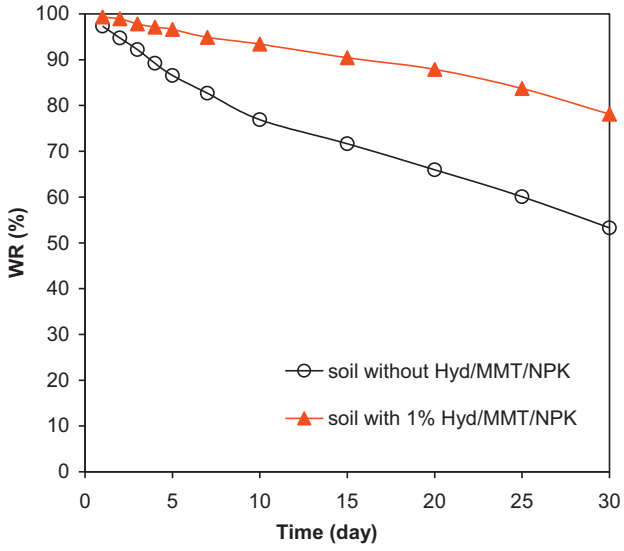

Fig. 7. Water-retention behaviors of the soil with and without Hyd/MMT/NPK

compositions already described in the literature (Guo et al., 2005; Liang & Liu, 2006). First, the preparation of formulation takes place in one step by in-situ polymerization in the presence of fertilizer. So, there is no need to additional steps for coating of fertilizer granules with superabsorbent nanocomposite. Furthermore, the use of montmorillonite is more advantageous from the economical point of view and also due to its water absorption ability. Therefore, the superabsorbent nanocomposite can not only absorb a large amount of water and preserve the soil moisture in arid areas but can also regulate the fertilizer release behavior.

The mechanisms of fertilizer release from Hyd/MMT/NPK superabsorbent nanocomposite using the kinetic release data of fertilizer in water and soil were analyzed applying Korsmeyer–Peppas and Higuchi models (Higuchi, 1963; Korsmeyer, Gurny, Doelker, Buri, & Peppas, 1983). From the results, the good fitness was found with higuchi and Korsmeyer–Peppas model for release into water and soil, respectively. This Fickian diffusion mechanism indicates that fertilizer diffuses partially through a swollen matrix and water filled pores in the prepared samples. The results are in conformity with the findings of previous work (Rashidzadeh et al., 2014) and other works (Jamnongkan & Kaewpirom, 2010), which showed that fertilizer release followed Fickian diffusion type transport mechanism. The detailed explanation of fertilizer release kinetics was provided in supplementary data.

3.5. Water retention behavior of Hyd/MMT/NPK in soil

Fig. 7 shows the water-retention behaviors of the soil with and without Hyd/MMT/NPK. From Fig. 7, we find that the addition of Hyd/MMT/NPK to soil could obviously increase the water-retention and decrease the water evaporation of the soil. The water retention ratio of soil without Hyd/MMT/NPK had only remained 71.64% and 53.27% on the 15th and 30th days, respectively, while that of the soil with Hyd/MMT/NPK was 90.44% and 78.09%, respectively.

4. Conclusions

A novel Hyd/MMT/NPK superabsorbent nanocomposite was successfully prepared by in-situ polymerization method in the presence of NPK fertilizer. The FTIR spectra indicated the incorporation of the montmorillonite within the superabsorbent matrix. The exfoliated structure of Hyd/MMT/NPK was observed by XRD technique. The highly porous structure of Hyd/MMT/NPK formed by addition of montmorillonite to the pure superabsorbent and that incorporation increased the water absorption of superabsorbent nanocomposite. Fertilizer slow release in distilled water and soil indicated that the fertilizer release properties of Hyd/MMT/NPK conformed to the standard of slow-release fertilizers. Finally the superabsorbent nanocomposite designed in this work not only has excellent slow-release property but has also a good water retention capacity, which can reduce loss of fertilizer and improve the utilization of water in agricultural applications.

Acknowledgements

The financial support of this work by the University of Tabriz is gratefully acknowledged.

Appendix A. Supplementary data

Supplementary data associated with this article can be found, in the online version, at http://dx.doi.org/10.1016/j.carbpol.2014.08.010.

References

Bajpai, A., & Giri, A. (2002). Swelling dynamics of a macromolecular hydrophilic network and evaluation of its potential for controlled release of agrochemicals. *Reactive and Functional Polymers*, *53*(2), 125–141.

Bao, Y., Ma, J., & Li, N. (2011). Synthesis and swelling behaviors of sodium carboxymethyl cellulose-*g*-poly (AA-*co*-AM-*co*-AMPS)/MMT superabsorbent hydrogel. *Carbohydrate Polymers*, *84*(1), 76–82.

Bortolin, A., Aouada, F. A., Mattoso, L. H., & Ribeiro, C. (2013). Nanocomposite PAAm/methyl cellulose/montmorillonite hydrogel: Evidence of synergistic effects for the slow release of fertilizers. *Journal of Agricultural and Food Chemistry*, *61*(31), 7431–7439.

Chaki, S., Deshpande, M., Tailor, J. P., Chaudhary, M. D., & Mahato, K. (2012). Growth and characterization of ADP single crystal. *American Journal of Condensed Matter Physics*, *2*(1), 22–26.

El-Rehim, A., & Hassan, A. (2006). Characterization and possible agricultural application of polyacrylamide/sodium alginate crosslinked hydrogels prepared by ionizing radiation. *Journal of Applied Polymer Science*, *101*(6), 3572–3580.

El-Rehim, H., Hegazy, E. S. A., & El-Mohdy, H. (2004). Radiation synthesis of hydrogels to enhance sandy soils water retention and increase plant performance. *Journal of Applied Polymer Science*, *93*(3), 1360–1371.

Emrani, A., Davoodnia, A., & Tavakoli-Hoseini, N. (2011). Alumina supported ammonium dihydrogenphosphate ($NH_4H_2PO_4/Al_2O_3$): Preparation, characterization and its application as catalyst in the synthesis of 1,2,4,5-tetrasubstituted imidazoles. *ChemInform*, *42*(46), no.

Guo, M., Liu, M., Hu, Z., Zhan, F., & Wu, L. (2005). Preparation and properties of a slow release NP compound fertilizer with superabsorbent and moisture preservation. *Journal of Applied Polymer Science*, *96*(6), 2132–2138.

Higuchi, T. (1963). Mechanism of sustained-action medication. Theoretical analysis of rate of release of solid drugs dispersed in solid matrices. *Journal of Pharmaceutical Sciences*, *52*(12), 1145–1149.

Hua, S., & Wang, A. (2009). Synthesis, characterization and swelling behaviors of sodium alginate-*g*-poly(acrylic acid)/sodium humate superabsorbent. *Carbohydrate Polymers*, *75*(1), 79–84.

Hussien, R. A., Donia, A. M., Atia, A. A., El-Sedfy, O. F., El-Hamid, A. R. A., & Rashad, R. T. (2012). Studying some hydro-physical properties of two soils amended with kaolinite-modified cross-linked poly-acrylamides. *Catena*, *92*, 172–178.

Jamnongkan, T., & Kaewpirom, S. (2010). Controlled-release fertilizer based on chitosan hydrogel: Phosphorus release kinetics. *Science Journal Ubonratchathani University*, *1*, 43–50.

Jung, Y. M., Czarnik-Matusewicz, B., & Kim, S. B. (2004). Characterization of concentration-dependent infrared spectral variations of urea aqueous solutions by principal component analysis and two-dimensional correlation spectroscopy. *Journal of Physical Chemistry B*, *108*(34), 13008–13014.

Korsmeyer, R. W., Gurny, R., Doelker, E., Buri, P., & Peppas, N. A. (1983). Mechanisms of solute release from porous hydrophilic polymers. *International Journal of Pharmaceutics*, *15*(1), 25–35.

Liang, R., & Liu, M. (2006). Preparation and properties of coated nitrogen fertilizer with slow release and water retention. *Industrial and Engineering Chemistry Research*, *45*(25), 8610–8616.

Liu, C.-H., Wu, J.-Y., & Chang, J.-S. (2008). Diffusion characteristics and controlled release of bacterial fertilizers from modified calcium alginate capsules. *Bioresource Technology*, *99*(6), 1904–1910.

Marandi, G. B., Mahdavinia, G. R., & Ghafary, S. (2011). Collagen-*g*-poly (sodium acrylate-*co*-acrylamide)/sodium montmorillonite superabsorbent nanocomposites: Synthesis and swelling behavior. *Journal of Polymer Research*, *18*(6), 1487–1499.

Muley, G. (2012). Study on growth habit, SHG and thermal properties of urea phosphate doped KDP crystals. *Science and Technology*, *2*(5), 109–113.
Ni, B., Liu, M., Lü, S., Xie, L., & Wang, Y. (2010). Multifunctional slow-release organic–inorganic compound fertilizer. *Journal of Agricultural and Food Chemistry*, *58*(23), 12373–12378.
Olad, A., & Rashidzadeh, A. (2012). Poly(*N*-vinylpyrrolidone) modified polyaniline/Na^+-cloisite nanocomposite: Synthesis and characterization. *Fibers and Polymers*, *13*(1), 16–20.
Owens, D. E., Jian, Y., Fang, J. E., Slaughter, B. V., Chen, Y.-H., & Peppas, N. A. (2007). Thermally responsive swelling properties of polyacrylamide/poly(acrylic acid) interpenetrating polymer network nanoparticles. *Macromolecules*, *40*(20), 7306–7310.
Pavlidou, S., & Papaspyrides, C. (2008). A review on polymer-layered silicate nanocomposites. *Progress in Polymer Science*, *33*(12), 1119–1198.
Pourjavadi, A., Ghasemzadeh, H., & Soleyman, R. (2007). Synthesis, characterization, and swelling behavior of alginate-*g*-poly(sodium acrylate)/kaolin superabsorbent hydrogel composites. *Journal of Applied Polymer Science*, *105*(5), 2631–2639.
Rahman, M., Das, B., Miah, M., & Ahmad, H. (2008). Fixation of urea to poly(acrylamide–maleic acid) and nitrogen release behaviour of the product—A comparison with urea and control. *Bulgarian Journal of Agricultural Science*, *14*(4), 373–380.
Rashidzadeh, A., Olad, A., Salari, D., & Reyhanitabar, A. (2014). On the preparation and swelling properties of hydrogel nanocomposite based on sodium alginate-*g*-poly(acrylic acid-*co*-acrylamide)/clinoptilolite and its application as slow release fertilizer. *Journal of Polymer Research*, *21*(2), 1–15.
Schexnailder, P., & Schmidt, G. (2009). Nanocomposite polymer hydrogels. *Colloid and Polymer Science*, *287*(1), 1–11.
Seetapan, N., Wongsawaeng, J., & Kiatkamjornwong, S. (2011). Gel strength and swelling of acrylamide–protic acid superabsorbent copolymers. *Polymers for Advanced Technologies*, *22*(12), 1685–1695.
Teodorescu, M., Lungu, A., & Stanescu, P. O. (2009). Preparation and properties of novel slow-release NPK agrochemical formulations based on poly(acrylic acid) hydrogels and liquid fertilizers. *Industrial and Engineering Chemistry Research*, *48*(14), 6527–6534.
Trenkel, M., & Association, I. F. I. (1997). *Stratospheric ozone*. London: HMSO.
Wang, Q., Hu, X., Du, Y., & Kennedy, J. F. (2010). Alginate/starch blend fibers and their properties for drug controlled release. *Carbohydrate Polymers*, *82*(3), 842–847.
Wang, Q., Zhang, N., Hu, X., Yang, J., & Du, Y. (2007). Alginate/polyethylene glycol blend fibers and their properties for drug controlled release. *Journal of Biomedical Materials Research, A*, *82*(1), 122–128.
Wang, Z., Nakajima, H., Manias, E., & Chung, T. (2003). Exfoliated PP/clay nanocomposites using ammonium-terminated PP as the organic modification for montmorillonite. *Macromolecules*, *36*(24), 8919–8922.
Wu, J., Wei, Y., Lin, J., & Lin, S. (2003). Study on starch-graft-acrylamide/mineral powder superabsorbent composite. *Polymer*, *44*(21), 6513–6520.
Wu, L., & Liu, M. (2007). Slow-release potassium silicate fertilizer with the function of superabsorbent and water retention. *Industrial and Engineering Chemistry Research*, *46*(20), 6494–6500.
Wu, L., & Liu, M. (2008). Preparation and characterization of cellulose acetate-coated compound fertilizer with controlled-release and water-retention. *Polymers for Advanced Technologies*, *19*(7), 785–792.
Zohuriaan-Mehr, M., Omidian, H., Doroudiani, S., & Kabiri, K. (2010). Advances in non-hygienic applications of superabsorbent hydrogel materials. *Journal of Materials Science*, *45*(21), 5711–5735.